CHAPTER 3

Effects of HTL and ETL Thicknesses on the Performance of PQT-12/PCDTBT:$PC_{61}BM$/ZnO QDs Organic Solar Cells

3.1 Introduction

In Chapter-2, we discussed the effect of FTM coated PQT-12 as an interface layer on the performance of ITO/ZnO QDs/PCDTBT:$PC_{61}BM$/PQT-12/PEDOT:PSS/Ag BHJ organic solar cells (OSCs). It was observed that the PQT-12 interface layer between the PCDTBT:$PC_{61}BM$ and PEDOT:PSS improved the performance over the device without the PQT-12 layer. It is reported that the use of PEDOT:PSS as the hole transport layer (HTL) degrades the performance of the OSCs [122], [123]. Thus, the FTM based PQT-12 may be used as a better replacement of PEDOT:PSS for the HTL due to its better stability [57] and energy band alignment with the PCDTBT than those of the PEDOT:PSS as discussed in Chapter-2.

The photovoltaic parameters such as open-circuit voltage (Voc), short circuit current density (Jsc), and fill factor (FF) are highly sensitive to the thicknesses of the electron transport layer (ETL) and HTL [124], [125]. In addition to the thicknesses, the deposition techniques used for the ETL and HTL also affect the performance of BHJ OSCs. The FTM has recently been successfully employed for fabricating low-cost, large-area, multi-layered devices [109], [110]. The FTM based PQT-12 films have been successfully used in the OSCs in Chapter-2. In this chapter, we have investigated the effects of the thicknesses of FTM derived PQT-12 based ETL and ZnO QDs based HTL on the performance of ITO/ZnO QDs/PCDTBT:$PC_{61}BM$/PQT-12/Ag BHJ OSCs. The ZnO QDs have been synthesized using the solution method and the floating-film transfer method (FTM) has been used for fabricating the PQT-12 based HTL as considered in Chapter-2. The outline of the rest of this chapter is given as follows:

Section 3.2 deals with the experimental details regarding the fabrication of the proposed ITO-coated glass/ZnO QDs/PCDTBT:$PC_{61}BM$/PQT-12/Ag based BHJ OSC. Section 3.3 comprises various results and discussions regarding electrical (J-V characteristic, Nyquist plot) and optical (absorption, external quantum efficiency) characterization. Finally, Section-3.4 summarizes the objectives and concludes the major observations of this chapter.

3.2 Experimental Details

3.2.1 Materials and Synthesis

The useful polymers, PQT-12, PCDTBT, $PC_{61}BM$, and other chemicals required for cleaning purposes were purchased already mentioned in Chapter-2. The ZnO QDs (~2.53 nm) were synthesized using the chemical solution method described in [101]. In short, zinc acetate dihydrate (precursor) was dissolved in 2-methoxy ethanol under a nitrogen environment until the temperature reached up to 65ºC. Now equivalent molar of monoethanolamine (MEA) as stabilizing reagent was injected in the solution and kept the resulting solution (of ZnO QDs) for 24 hours at room temperature. The prepared ZnO QDs solution was then filtered by using a 0.22 µm PVDF filter to remove any unreacted part.

3.2.2 Solar Cell Fabrication

The BHJ OSCs were made on cleaned ITO coated glass substrate in an open-air environment (without using a glove box) unless any specific condition was mentioned. The ZnO QD was spin-coated at 3000 rpm for 30 s on cleaned ITO glass substrate and then heated at 150ºC for preparing ETL. Finally, the ETL was annealed at 200ºC for 30 minutes in an ambient environment to act as the ETL. To prepare the organic active layer, 5 mg of PCDTBT in 1 ml dichlorobenzene and the solution was stirred at 60ºC for nearly 10 hours. After that 15 mg of PC_{61}BM was mixed into PCDTBT solution and then stirred for uniform mixing for 2 hours prior to final deposition. The resultant PCDTBT:PC_{61}BM solution was spin-coated on the previously deposited ZnO QDs based ETL layer at 1500 rpm for 50 seconds and then annealed at 120ºC for 30 minutes in an argon environment to fabricate the active layer (~110 nm).

The PQT-12 film was then deposited for HTL on the active layer by the FTM technique [114], [126], [127] as demonstrated in Figure 3.1 (a). In brief, PQT-12 hydrophobic solution (in chloroform) was dispersed on the hydrophilic solution of ethylene glycol and glycerol (prepared in 1:1 ratio) in a petri dish. The dispersed PQT-12 film was then stamped on the hydrophobic surface of the active layer. The good adhesive nature of the active layer to PQT-12 ensures a good active layer/HTL interface [114], [126]. The samples were finally dried up by heating at 120°C for 10 min in an argon environment. Now finally, the shadow masking technique was used to fabricate 100 nm silver (Ag) metal dots of 2 mm diameter on the HTL for the top electrode by a thermal evaporation method (Model no. FL400 SMART COAT 3.0 A from HHV, India).

The energy band diagram for the fabricated OSCs structure is shown in Figure 3.1 (b). It is observed from Figure 3.1 (b) that the band alignment of PQT-12 based HTL with the active layer is assisted with the separation of electron-hole pairs in the active layer that reduces recombination. Clearly, FTM-based PQT-12 film serves as an efficient HTL in the OSCs structure. The cross-sectional image of the fabricated optimized structure without the Ag electrode is shown in Figure 3.2. The complete schematic of the proposed BHJ OSCs is shown in the inset of Figure 3.2. Four fabricated OSCs samples with fixed HTL thickness of 20 nm but with different ETL thicknesses of 20 nm, 25 nm, 30 nm, and 35 are denoted by ZnO (20), ZnO (25), ZnO (30), and ZnO (35), respectively. The performance of the solar cells is reported to be degraded with increased ZnO based ETL thickness due to increase in the contact resistance between ZnO layer and active layer [125]. That is why, we have restricted the ETL thickness up to 35 nm only. On the other hand, three OSCs with a fixed ETL thickness of 20 nm but with three different HTL thicknesses of 20 nm, 40 nm, and 60 nm are denoted by PQT-12 (20), PQT-12 (40), and PQT-12 (60), respectively.

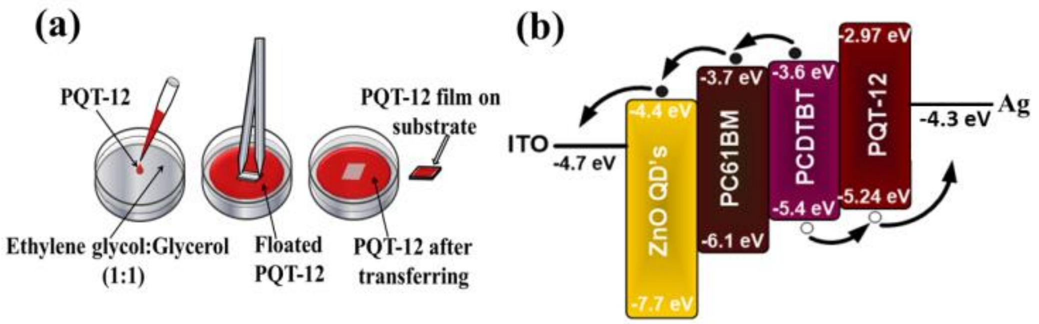

Figure 3.1: (a) FTM deposition steps for PQT-12 film and (b) Energy band diagram for the OSCs structure.

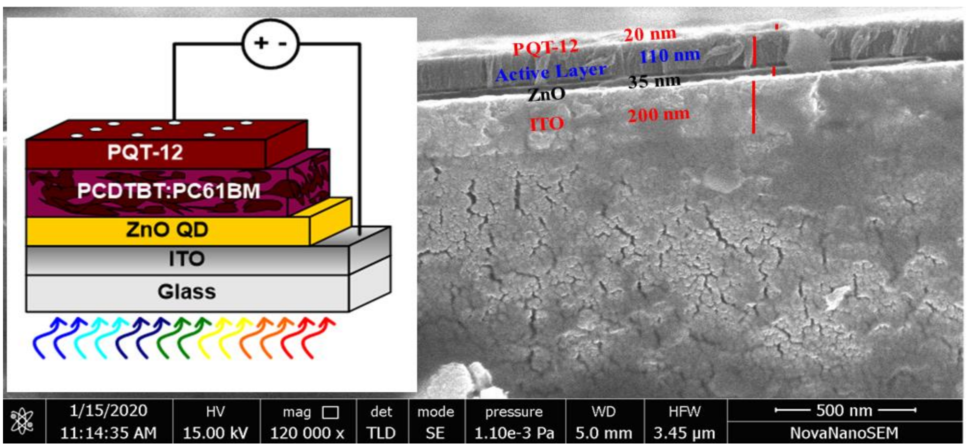

Figure 3.2: HRSEM cross-sectional image of the optimized OSC structure without Ag and complete OSC device structure in the inset.

3.3 Results and Discussion

In this section, optical as well as electrical characterizations of the fabricated BHJ OSCs have been discussed in detail.

3.3.1 Optical Characterization

The absorbance spectra of the PCDTBT:$PC_{61}BM$ based active layer and PQT-based HTL are shown in Figure 3.3. Figure 3.3 shows significant absorption of the visible spectrum in the active layer. The absorption of a part of the visible spectrum also takes place in the HTL. Thus, the active layer along with the HTL enhances the overall optical absorption in the visible spectrum. The transmittance spectra of the ZnO QDs based ETL are shown in Figure 3.4 for different thicknesses. The ETL appears to be nearly transparent (> 80%) in the visible range. This ensures that the significant part of the visible light enters into the active layer to contribute photocurrent in the device. However, light reduction in the transmittance with increased ETL thickness may be attributed to increased reflectance at higher wavelengths due to the plasma resonance of electron gas in the conduction band of the active layer [128].

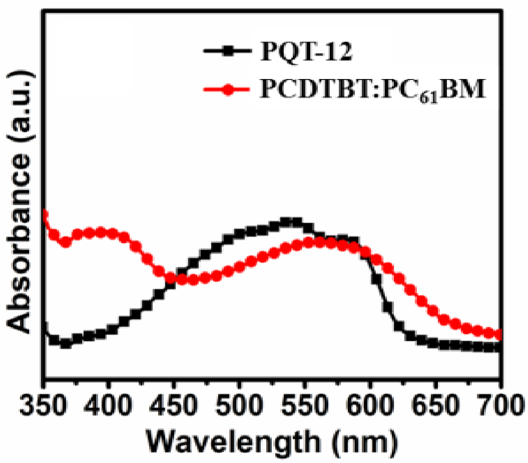

Figure 3.3: Absorbance of PQT-12 and PCDTBT:$PC_{61}BM$ film.

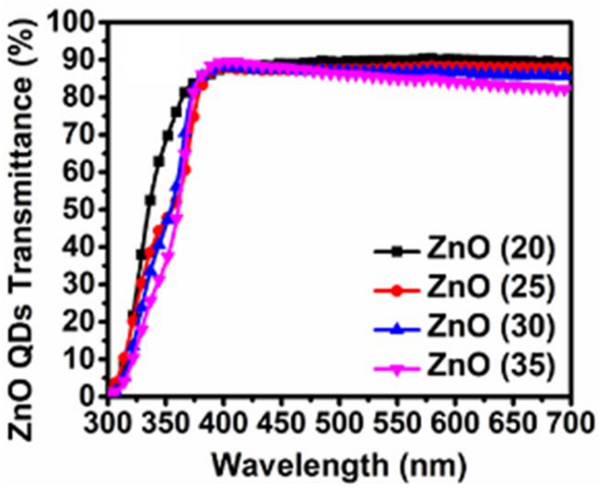

Figure 3.4: Transmittance of ZnO QDs thin film with different thicknesses.

The external quantum efficiency (EQE) calculated from the *J*-λ characteristics [129], which is measured using the monochromator unit (Model No. SP2150i from Princeton Instruments, USA) and attached halogen light source have been shown for different HTL thicknesses in Figure 3.5 and for different ETL thicknesses in and Figure 3.6. Since the absorptions in HTL and ETL regions also contribute to the photocurrent to some extent, the EQE peaks are observed to be red-shifted slightly with increased HTL and ETL thicknesses. The OSC with 20 nm HTL thicknesses and 35 nm ETL thicknesses shows the highest EQE among all the samples under study.

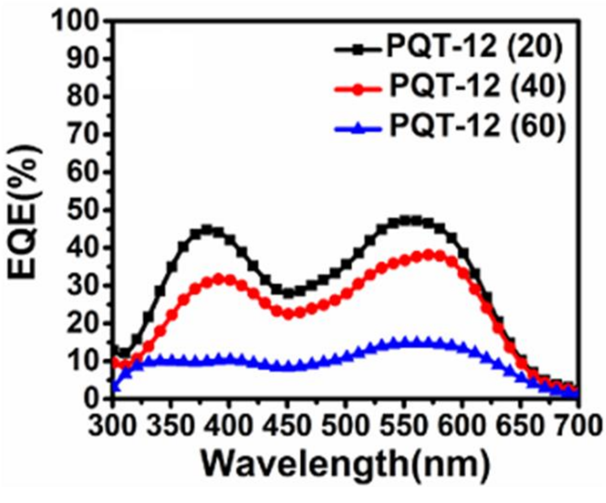

Figure 3.5: EQE characteristics for different HTL thicknesses with fixed ZnO of 20 nm.

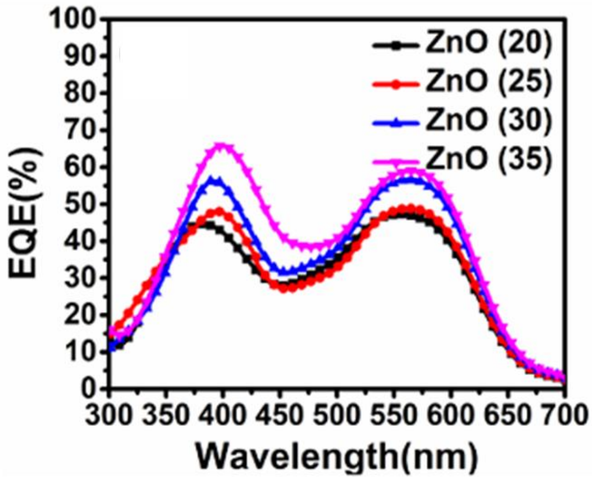

Figure 3.6: EQE characteristics for different ETL thicknesses with fixed PQT-12 of 20 nm.

3.3.2 Electrical Characterization

The current densities (J) vs. voltage (V) characteristics of OSCs under one sunlight are measured by a parameter analyzer (Model No. B1500A from Keysight, USA) in ambient open-air conditions. The standard solar light spectrum has been obtained using the solar simulator (Model SS50AAA from Photo Emission Technology, USA), which is calibrated for AM 1.5 G standard sunlight with a light intensity of 100 mW/cm^2 using a standard reference cell (Model No. 60623 from National Renewable Energy Laboratory, USA). The measured *J-V* characteristics of PQT-12 (20), PQT-12 (40), and PQT-12 (60) are shown in Figure 3.7. The PQT-12 (20 nm) based OSC shows the highest J_{SC} of 6.62 mA/cm^{2,} whereas the J_{SC} of PQT-12 (40 nm) and PQT-12 (60 nm) samples are 5.86 mA/cm^2 and 2.94 mA/cm^2, respectively. The values of other parameters with the variable thickness of PQT-12 are summarized in Table 3.1. The PCE and fill factor can be improved further by carrying out the fabrication and characterization of the OSCs in a controlled environment using a glove box. It is found that the PCE deteriorates with the increase in the PQT-12 based HTL thickness due to a reduction in hole transfer rate through the HTL.

Table 3.1: Photovoltaic Parameters with Varying PQT-12 Thickness

S.No.	PQT-12 (nm)	ZnO (nm)	J_{sc} (mA/cm^2)	V_{oc} (mV)	FF (%)	PCE (%)
1	20	20	6.62	566	28	1.05
2	40	20	5.86	495	29	0.84
3	60	20	2.94	612	27	0.49

Table 3.2: Photovoltaic Parameters with Varying ZnO QDs thickness

S.No.	PQT-12 QD (nm)	ZnO (nm)	J_{sc} (mA/cm^2)	V_{oc} (mV)	FF (%)	PCE (%)
1	20	20	6.62	566	28	1.05
2	20	25	6.85	602	32	1.31
3	20	30	9.44	656	35	2.16
4	20	35	10.42	672	38	2.66

The effect of ETL thickness for a fixed HTL thickness of 20 nm the *J-V* characteristics of OSCs are shown in Figure 3.8. The Figure shows that J_{SC} is increased with the ZnO QDs based ETL thickness. Almost more than 80 % transmittance is shown by the various thickness of ZnO shown in Figure 3.4; therefore, a similar amount of visible light will reach even with increasing thickness of ZnO. The variations in the other parameters of the OSCs are listed in Table 3.2. The maximum PCE of 2.66% is obtained for the OSC with 35 nm ETL thickness and 20 nm HTL thickness. The increased PCE with ETL thickness may be attributed to the enhanced charge transport as well as charge extraction in the OSCs [125]. Improved charge transportation and extraction with increased ZnO QDs based ETL thickness reduce the recombination, which, in turn, enhances the dissociation of more photo-generated electron-hole pairs into electrons and holes. Enhanced numbers of dissociated photo-generated electrons and holes move toward their respective electrodes to improve the performance of the BHJ OSCs.

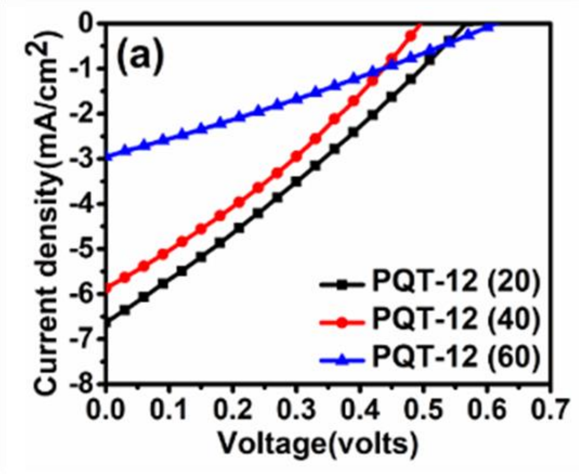

Figure 3.7: J-V characteristics of solar cells for fixed ETL thickness of 20 nm and different PQT-12 thicknesses of 20 nm, 40 nm, and 60 nm.

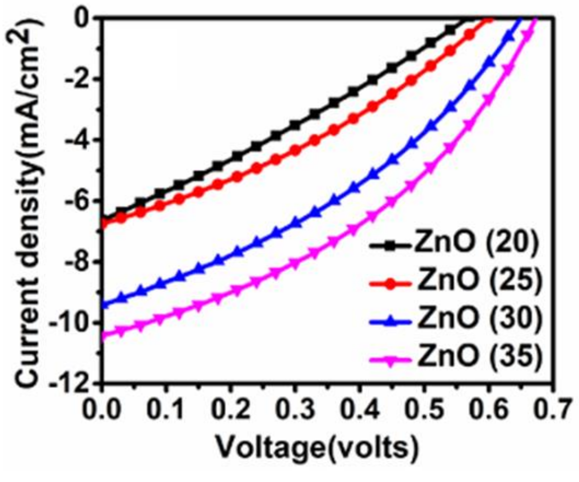

Figure 3.8: J-V characteristics of solar cells for a fixed PQT-12 based HTL thickness of 20 nm with four different ZnO QDs based ETL thicknesses of 20 nm, 25 nm, 30 nm, and 35 nm.

To analyze the stability of the proposed OSC in the ambient air conditions, the J-V characteristics of the OSC (with PQT-12 layer thickness of 20 nm and ZnO QDs layer thickness of 35 nm) are measured every day for a period over 7 days after the fabrication of the device. The results are shown in Figure. 3.9. Day-wise performance parameters are shown in Table 3.3. About 11.36% degradation in the PCE is observed after 7 days in open environments. The performance degradation can be prevented by proper packaging of the device.

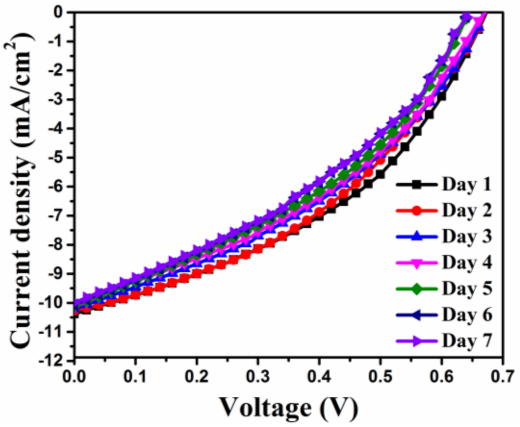

Figure. 3.9. J-V characteristics of device with 20 nm and 35 nm of PQT-12 and ZnO QDs, respectively to realize seven days stability.

Table. 3.3. Seven days analysis of the device with 20 nm and 35 nm of PQT-12 and ZnO QDs, respectively.

S.No	Days	Jsc (mA/cm^2)	Voc (mV)	FF (%)	PCE (%)
1	Day 1	10.38	670	38	2.64
2	Day 2	10.27	670	38	2.61
3	Day 3	10.20	668	37	2.52
4	Day 4	10.14	668	37	2.50
5	Day 5	10.10	644	36	2.34
6	Day 6	10.05	642	36	2.32
7	Day 7	10.00	642	36	2.31

We will now consider the impedance analysis in the 1 kHz -1 MHz frequency range at respective open-circuit voltages of OSCs under solar illumination. The Nyquist plots for different HTL and ETL thicknesses are shown in Figure 3.10 and Figure 3.11, respectively. The decreased diameter of semicircles with reduced (enhanced) HTL (ETL) thickness implies that the charge transportation (and hence the mobility) can be improved by reducing (increasing) the HTL (ETL) thickness [130]. In brief, an increase (decrease) in ETL (HTL) thickness thus reduces the recombination and enhances charge transportation in the active layer. Thus, the results of Figure 3.10 and Figure 3.11 confirm that the OSC with HTL thickness of 20 nm and ETL thickness of 35 nm possesses the highest performance among all the OSCs under study. The results of Figure 3.10 and Figure 3.11 also agree with the *J-V* and EQE analysis.

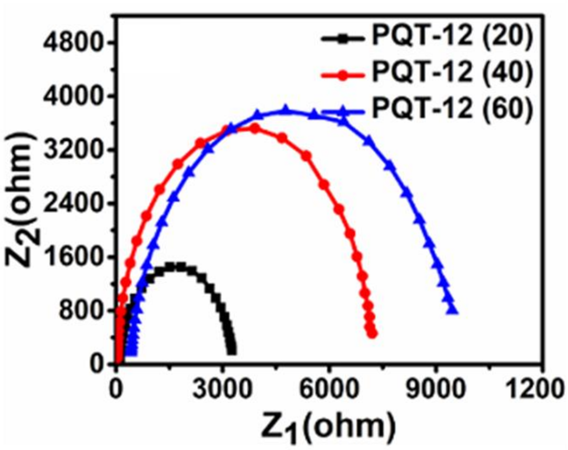

Figure 3.10: Nyquist plot with variation in PQT-12 thickness with fixed ZnO QDs of 20 nm.

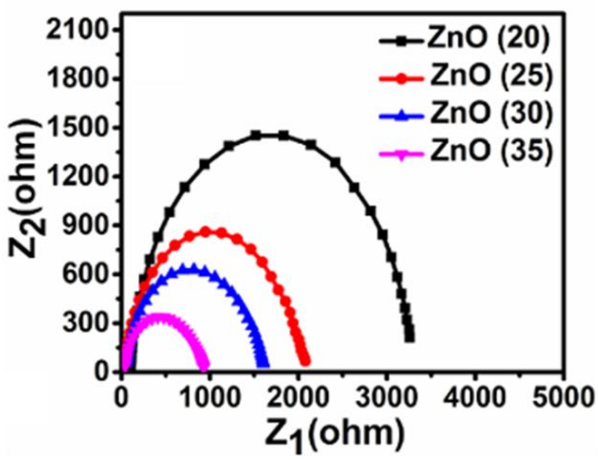

Figure 3.11: Nyquist plot with variation in ZnO QDs thickness with fixed PQT-12 of 20 nm.

3.4 Conclusion

The effects of ZnO QDs based ETL and FTM transferred PQT-12 film based HTL thicknesses on ITO/ZnO QDs/PCDTBT:$PC_{61}BM$/PQT-12/Ag structured BHJ solar cells have been investigated in this chapter for the first time. It is observed that a better PCE can be obtained for smaller HTL thickness and larger ETL thickness of the OSCs. Three OSCs with three different HTL thicknesses of 20 nm, 40 nm, and 60 nm but with a fixed ETL thickness of 20 nm fabricated to investigate the effects of the FTM transferred PQT-12 film based HTL thickness on the performance of the solar cells under study. On the other hand, four OSCs with a fixed HTL thickness of 20 nm but four different ETL thicknesses of 20 nm, 25 nm, 30 nm, and 35 nm are used for studying the effect of ETL layer thickness on the PCDTBT:$PC_{61}BM$ based BHJ OSCs. The OSC with ~20 nm thin PQT-12 based HTL and ~35 nm thin ZnO QDs based ETL shows the highest performance parameters with J_{SC}, V_{OC}, and PCE of 10.42 mA/cm^2, 672 mV, and 2.66%, respectively. The present study can be used for the optimization of the other BHJ OSCs by optimizing the ETL and HTL layer thicknesses of the device.